

PICKED FEL MICROPULSE FOR NANO-SECOND INTERACTION WITH BIO-MOLECULE

S. Y-Suzuki*, T. Kanai, K. Ishii, Y. Naito, K. Awazu, Institute of Free Electron Laser, Graduate School of Engineering, Osaka Univ., 2-9-5 Tsuda-yamate, Hirakata, Osaka 573-0128, Japan

Abstract

Laser pulse duration is a very important parameter to determine the threshold between thermal and nonthermal effects in laser surgery of biomedical tissue. Free Electron Laser (FEL) at Osaka University, Japan, has a pulse structure in which a macropulse (pulse width: 15 μ s) consists of equally separated micropulses, whose width and interval are approximately 5 ps and 44.8 ns, respectively. A precisely controlled of micropulse train may establish fast optic processes because thermal relaxation time in tissue is about 1 μ s. A pulse-picking system was designed in order to extract a single or a few micropulses from an entire macropulse using an acousto-optic modulator (AOM) in which the light path can be transiently diffracted by an external gate signal. The extracted micropulse train was monitored by a mercury-cadmium-telluride (MCT) photodetector with \sim 1 ns response time and recorded on a digital oscilloscope. A single micropulse was extracted as a result of adjusting the duration of the gate signal to 50 ns which is nearly equal to the micropulse interval. Investigation of a fast interaction between FEL and tissue using this system is expected.

INTRODUCTION

Many bio-molecules absorb mid-infrared (MIR) light strongly due to molecular vibration. Exciting a specific molecular vibration selectively using MIR pulse laser gives various medical treatment effects on a level of molecules.

In laser surgery, controlling thermal effects is important. The thermal and nonthermal effects are generally classified according to the thermal relaxation time (τ_{therm}) of a biomedical tissue. If the interaction time (τ_{int}) which depends on the pulse width and frequency of laser is longer than the thermal relaxation time ($\tau_{\text{int}} > \tau_{\text{therm}}$), the heat spreads over the entire biomedical tissue and produces macroscopic thermal effects. For example, a surgical laser incision and coagulation in tissue using the thermal effect. However, the thermal effect has an influence on normal tissue due to diffusion, and the selective interaction by bio-molecular vibration is not expectable. In the case of $\tau_{\text{int}} < \tau_{\text{therm}}$, because a particular molecule is excited within τ_{therm} , the selective interaction is caused faster than diffusion.

Biomedical applications have been studied using a free electron laser (FEL). FEL at iFEL, Osaka University in JAPAN, is tunable from 5 μ m to 22 μ m in mid-infrared

(MIR) region, which is high peak power and short pulse operation. The FEL has a unique double pulse structure; the structure consists of a train of macropulses, and each macropulses contains an ultrashort 300-400 micropulses. The width of a macropulses is about 15 μ s and repetition rate is 10 Hz. The width of a micropulse is shorter than 10 ps and the separation between micropulses is 44.8 ns. Therefore, precise control of micropulses is required in order to evaluate FEL irradiation effects on the bio-molecule without thermal effects.

There is a number of technologies for switching the laser beam, e.g. Pockels cell (PC) [1, 2] or acousto-optic modulator (AOM). PC switches the polarization direction of laser beam rapidly by high-voltage switching. Becker *et al.* have achieved switch out from 80ns to the full 6 μ s duration of the FEL macropulse [1]. AOM can transiently diffract the light path with an external gate signal. The switching speed of AOM is slower than PC, but has a higher switching efficiency. We have chosen AOM control micropulse train.

A micropulse-picking apparatus was designed to switch-out a short micropulse train from an entire macropulse by a deflection of the light path using a germanium acousto-optic modulator (Ge-AOM). We will discuss the nano-second interaction with bio-molecular tissue sample.

PULSE-PICKING SYSTEM

Principle of the acousto-optic modulator

The basic principle of the acousto-optic modulator (AOM) is shown in figure 1. All AO devices are based on a crystalline material whose one side is bonded to a piezo-electric transducer. When radio frequency (RF) signal is applied to the transducer, an acoustic wave (AW) is produced by the inverse piezoelectric effect and travels in the crystal. The wave of condensation and rarefaction in the crystal is acted as a diffraction grating. An incident beam to the crystal is diffracted into many orders during the formation of the AW. If the angle of incidence is set to the Bragg angle, the majority of the diffracted light appears in the first order. This is the optimal setting in most practical application.

The Bragg angle (θ_B) is determined by wavelength of incident laser λ_i and RF drive frequency f_c .

$$\theta_B = \frac{\lambda_i f_c}{2 \cdot v} \quad (1)$$

, here v is velocity of AW into the crystal.

* suzuki@fel.eng.osaka-u.ac.jp

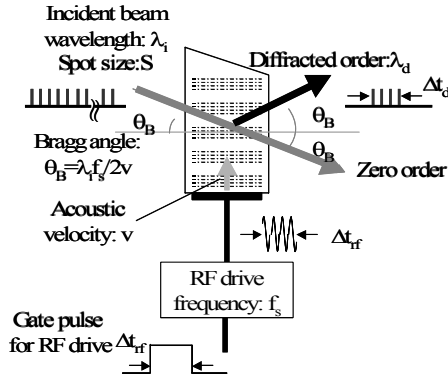


Figure 1: Basic principle of the acousto-optic modulator

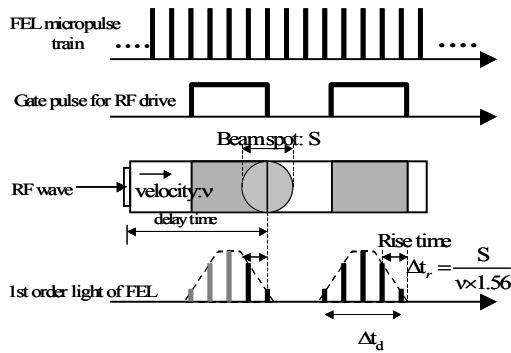


Figure 2: Time chart of pulse diffraction

Figure 2 shows a time chart and image of the pulsed diffraction. The diffracted light is produced while the pulsed AW passes the whole incident light spot. In other words, an adjustment of the gate pulse for the RF driver (Δt_{rf}) can control the micropulse train which is extracted from a macropulse. The minimum temporal window of the diffracted light (Δt_d) is limited by the rise / fall time (Δt_r) which depends on the AW velocity (v) and light spot size (S).

$$\Delta t_r = \frac{S}{v \times 1.56} \quad (2)$$

(1.56=a correction factor for large beam size)

Designs

The setup for diffraction of FEL beam is shown in figure 3. As the crystalline material of AOM, we chose a germanium (Ge-AOM) which has a high transmission and allowable input energy at MIR wavelength region. Table 1 shows the specification and the basic performance of the Ge-AOM (AGM-402A1, IntraCation CO.) and RF driver (GE-4010, IntraCation CO.) used in our experiments. We chose the Ge-AOM with anti-reflection (AR) coatings limited to 5.7~7.0 μm in order to eliminate the Fresnel reflection on the Ge surface.

In order to extract a signal or a few micropulses from an entire macropulse, the incident FEL beam spot size needs to be about 250 μm which is estimated from the equation (2) as equivalent to $\Delta t_d = 50$ ns. The focusing of FEL beam on AOM causes various problems; for example, damage to Ge and decrease in the diffraction efficiency. Therefore, the incident beam to AOM is better to be collimated.

The FEL beam which was focused with two ZnSe convex lenses ($f_1 = 50$ cm, $f_2 = 3$ cm) entered the Ge-AOM at the Bragg angle ($\theta_B = 38.5$ mm radian). The polarization direction of the incident beam was vertical to the diffraction grating in the operating AOM. If the polarization is parallel to the gating, the diffraction efficiency is significantly reduced by the consequence of Maxwell equations. The diameter of incident beam is about 1 mm; it is too large to extract a single micropulse. However, it is possible to evaluate an interaction without the thermal effect in bio-medical tissue. Although the beam is not collimated, it is equivalent to the parallel light within the AOM because the beam divergence at an angle of 7 mm radian is smaller enough than the Bragg angle.

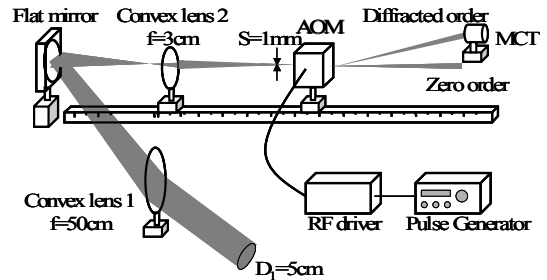


Figure 3: The setup for micropulse-picking

Table 1: specification and the basic performance of AOM and RF drive

Acousto-optic modulator (AGM-402A1)	
Acousto-optic material	Germanium
Acoustic Velocity (v)	5.5 mm/ μsec
RF Center Frequency	40 MHz
Optical Insertion Loss	< 7 percent
Optical wavelength	10.6 μm
Beam Separation	77 mm radian
Bragg Angle	38.5 mm radian
Diffraction Efficiency	70 percent
RF driver (GE-4010)	
Oscillator Frequency	40 MHz
RF Output Power	10 watts
Rise/Fall Time	30 nsec

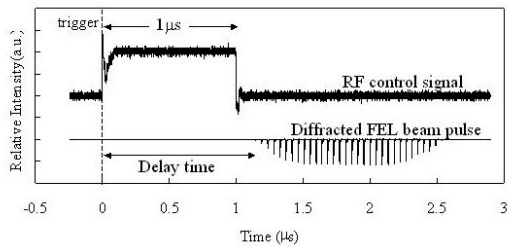


Figure 4: Experiment result of micropulse train extracted with the control signal of 1 μ s.

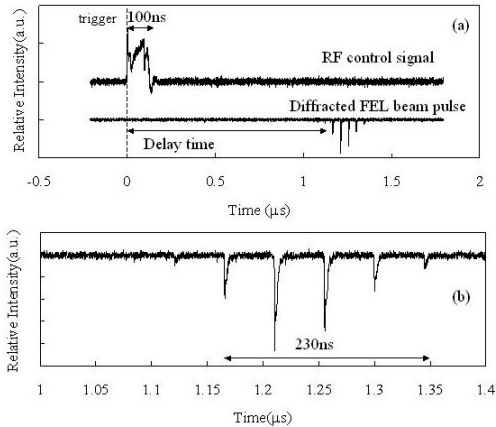


Figure 5: Experiment result of micropulse extracted with the control signal 100ns (a) and expansion of extracted micropulse (b).

RESULTS OF MICROPULSE EXTRACTION

Figure 4 and 5 show the results of the experiment for examination of the pulse-picking system using Ge-AOM. The temporal window for the micropulse-picking depends on the gate pulse for the RF driver. Figure 4 confirmed that about 30 micropulses ($44.8 \text{ ns} \times 30 = \sim 1.3 \mu\text{s}$) are extracted from an entire macropulse by the gate pulse of $\Delta t_{\text{rf}} = 1 \mu\text{s}$. The diffracted light was detected about $1.2 \mu\text{s}$ after the rising edge of the gate pulse. This delay time is caused by the response time (30ns) of the RF driver and the travel time of AW in the crystal. Figure 5 shows the micropulse train extracted by the gate pulse of $\Delta t_{\text{rf}} = 100 \text{ ns}$. Figure 5 (b) is the enlarged view. Five micropulses ($44.8 \text{ ns} \times 5 = \sim 230 \text{ ns}$) are found to be extracted and the picking temporal window Δt_{d} is different from Δt_{rf} . The window is limited to the rise time (t_r) of the AOM. In the case of the incident beam of 1 mm in diameter $t_r = 116 \text{ ns}$ is estimated from the equation (2). Therefore, a micropulse train of less than 232 ns cannot be extracted. Furthermore, in the case of $\Delta t_{\text{d}} < 232 \text{ ns}$, the diffracted light intensity decreased because the pulsed AW became not able to cover the entire incident beam spot and a portion of the incident light was

diffracted. This system can adjust the micropulse train in the range from 5 to 335 micropulses (macropulse width: 232 ns - 15 μs).

Figure 6 shows the optical insertion loss of wavelength 5~12 μm . The loss in the AR coatings wavelength region is about 7%, which agrees with the specification values. The loss in the region out of the AR coating wavelength ($< 10 \mu\text{m}$) is also low; it is less than 30%. The diffraction efficiencies at the FEL wavelength of 6.3 μm and 9.4 μm are 65~70%, also agree with specification value (see table 1).

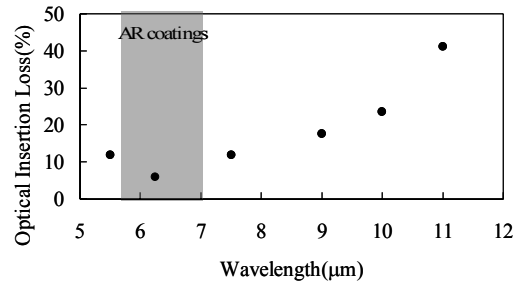


Figure 6: Optical insertion loss as a function of wavelength.

APPLICATIONS OF PICKING SYSTEM

Interaction with biomedical tissue

We have researched various interactions between biomedical tissues and MIR-FEL, for example the selective removal of cholesterol ester (5.75 μm), the surface modification of tooth dentin (9 μm band) and the control of dephosphorylation (9 μm band). Control of thermal effects is important to lead to these processes effectively.

We showed that the infrared absorption peak of the phosphate group is reduced after the FEL wavelength 9.4 μm irradiation (average power density 8.6 W/cm^2) [3]. The thermal effect on the interaction between a critical tissue and the controlled micropulse train was investigated. The length of the micropulse train was varied by the pulse-picking system while the average irradiation power density was adjusted to be constant. polyacrylic acid without phosphorylation was used as the sample in the primary experiment. polyacrylic acid is used as a model of a biomechanical material because chemical structure is simplicity and handling is easy. The sample was irradiated with FEL (wavelength 9.4 μm) of macropulse width of 15 μs and 2 μs respectively. Each irradiation effect is estimated by comparing the absorption spectra measured by Fourier Transform Infrared Spectrometer (FT-IR). When an entire macropulse is irradiated (15 μs), the polyacrylic acid dissolved remarkably. In contrast, the decrease in micropulse train ($\sim 2 \mu\text{s}$) reduces thermal effect and the chemical structure is kept. Evaluate of interaction which controlled thermal effect is expected.

Matrix-assisted laser desorption/ionization using UV laser and FEL

Matrix-assisted laser desorption/ionization (MALDI) is a powerful and robust technique for protein identification [4]. We have developed a novel MALDI method based on a simultaneous irradiation of a UV laser and FEL (UV/FEL-MALDI). The UV laser and FEL can create electronically and vibrationally excited states on a sample in parallel. The results provided analyses of macromolecules and insoluble proteins which are not amenable to the conventional measurement [5, 6].

The typical pulse width for MALDI has been reported to be ~ 100 ns, however neither of macropulse nor micropulse of our FEL has a suitable time scale. To achieve the optimum irradiation condition, the FEL micropulse train and the timing of electronic and vibration excitation need to be adjusted arbitrarily.

Figure 8 shows a schematic diagram of UV/FEL-MALDI time-of-flight mass spectrometer (TOF-MS) with a micropulse picking system. The irradiation of the UV laser and FEL is controlled by synchronous trigger signals. Figure 9 shows the timing chart of the irradiation event. This result confirms that the diffracted FEL micropulse train and UV laser pulse are irradiated simultaneously. The UV/FEL-MALDI with the micropulse picking system which extracts a short micropulse train can synchronize precisely the UV and FEL laser pulses and is expected to elucidate the ion generation mechanism and to improve the efficiency of ionization.

CONCLUSIONS

In order to control the FEL micropulse train for classifying thermal and non-thermal effects on biomedical tissue, we designed a micropulse picking system using Ge-AOM in which the light path can be diffracted to extract a few micropulses from an entire macropulse. The pulse-picking system achieved to control the diffracted micropulse train from 232 ns to 15 μ s. The diffraction efficiency reached to 65~70%.

The thermal effect related to the interaction between a micropulse train and phosphorylate acrylamide was verified. The result obtained by the controlled micropulse train, whose length was varied at the constant average power, confirmed that limiting the micropulse train decreases the thermodiffusion in a critical tissue. The UV/FEL-MALDI equipped with the picking system can control the timing of electronic and vibration excitation precisely, and many achieve the optimum irradiation condition for protein identification. The picking system is expected to give many information about interaction between laser and biomedical tissue.

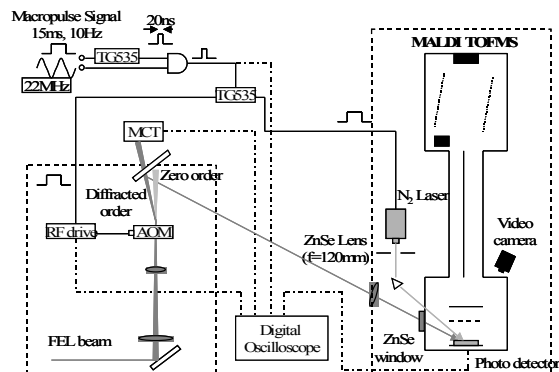


Figure 8: UV/FEL-MALDI TOFMS required micropulse-picking system.

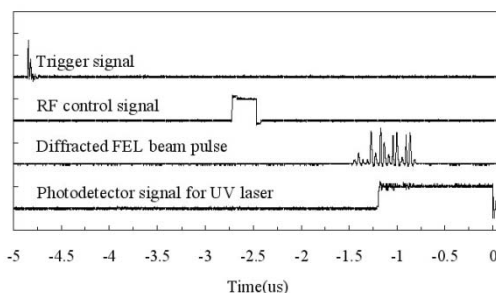


Figure 9: Experiment result of timing control on a simultaneous irradiation of a UV laser and FEL.

ACKNOWLEDGMENTS

We are grateful to Mr. Kuma, Mr. Marusaki and Mr. Teranishi, operational staff of iFEL graduate school of engineering, Osaka University.

This study was supported by a research budget of the Intellectual Cluster Project from Senri Life Science Foundation / the Ministry of Education, Culture, Sports, Science and Technology of Japan.

REFERENCES

- [1] K. Becker et al., Rev. Sci. Instrum. 65(5), 1496(1994).
- [2] A. V. V. Nampoothiri et al., Rev. Sci. Instrum. 69(3), 1240(1998).
- [3] K. Ishii et al., Nucl. Instrum and Math. Phys. Res. A, 528, 614, (2004).
- [4] K. Tanaka et al., Rapid Commun. Mass Spectrometry, 151(1998).
- [5] Y. Naito et al., Nucl. Instrum and Math. Phys. Res. A, 528(1-2), 609,(2004).
- [6] S. Y. Suzuki et al., Rev. Laser Engineering, 31(12), 835(2003).